ISSN NO. 2320-5407

Journal homepage: http://www.journalijar.com

INTERNATIONAL JOURNAL OF ADVANCED RESEARCH

RESEARCH ARTICLE

Photo induced interaction between magnetite Fe_3O_4 nanoparticles and Cisplatin anticancer drug

Maged El-Kemary[1,*], Tarek Fayed, [2], Eman A khalil[1,2],

1. Nanotechnology center, Faculty of Science, Kafrelsheikh University, 33516 KafrElSheikh, Egypt

2. Chemistry Department, Faculty of Science, Tanta University, Tanta, Egypt

Manuscript Info

Manuscript History:

Received: 22 May 2015
Final Accepted: 19 June 2015
Published Online: July 2015

Key words:

Environmental, Brucellosis, Patients, Rose Bengal test, Culture.

Corresponding Author

Maged El-Kemary

Abstract

Synthesis of magnetite (Fe_3O_4) nanoparticles (NPs) by simple preparation method. The structure of the synthesized Fe3O4 NPs is investigated by X-ray diffraction, fourier transform infrared (FT-IR) spectroscopy, thermal gravimetric analysis (TGA), and transmission electron microscopy (TEM). The results showed the crystallinity of Fe_3O_4 NP with a spherical shape. The synthesized Fe_3O_4 NPs have a diameter of ~ 14.8 nm.

INTRODUCTION

Magnetic and superparamagnetic NPs have been considered as effective contrast agents [1–3], which have been used as nanocarriers for specific delivery of chemotherapy agents [4–6]. Magnetite is an important type of magnetic material, having a cubic inverse spinel structure, and has been the subject of increasing attention because of its use in magnetic recording tape, [7] ferrofluid, [8] catalysts,[9] and biomedical applications, such as magnetic resonance [10,11], bioseparation,[12,13] drug targeting, [14,15] and hyperthermia [13–16]. The magnetite can be synthesized by various methods, including: ultrasound irradiation [17], sol-gel [18], thermal decomposition [19–24] and co-precipitation [25-31]. Thermal decomposition and co-precipitation are most commonly used. Cisplatin is a platinum-based molecule widely used in the treatment of various forms of cancer in humans. **At this study** showing the effect of adding magnetite nanoparticles with different concentrations. studing type of reaction is also included.

2.Experimental

2.1. Chemicals

Ferric chloride hexahydrated 99% ($FeCl_3$.6H2O), ferrous chloride tetra hydrated 99% ($FeCl_2.4H_2O$), ammonia solution 32% (NH_4OH), ethanol 99%, and cisplatin (WAKO Japan 99%). All chemicals are of reagent grade and used without further purification. Water used in experiments was purified with Millipore system.

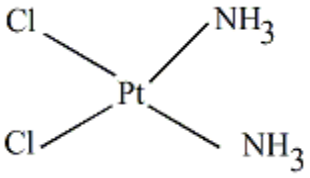

Scheme (1) Cisplatin anticancer drug.

2.2.a Preparation of magnetite nanoparticles Fe_3O_4:

For the synthesis of pure Fe_3O_4 nanoparticles, 1.99 gm of $FeCl_2.4H_2O$ and 3.24 gm of $FeCl_3$ with a molar ratio 1:2 respictevly were dissolved in 50 ml of distilled water. 30 ml of NH_4OH 32% was also dissolved in 50 ml of distilled water. In order to uniform mixing of the particles, both the solutions were allowed to stir for about half an hour. Then, the NH_4OH solution was added drop wise into the first solution till pH = 9. After the required pH is reached, the solution was kept under stirring. Then the solution was kept under sonication for about half an hour and the precipitates were obtained by repeated cycles of centrifuging in distilled water. The obtained precipitate was dried at 120º C for about 2 hrs and then grinded. The chemical reaction for Fe_3O_4 formation may be written as;

$$Fe^{2+} + Fe^{3+} + 8OH^- \rightarrow Fe_3O_4 + 4H_2O$$

2.2.b Sample preparation for fluorescence measurement

Stock solution of cisplatin anticancer drug 41 $x10^{-3}$ M in dimethyl sulfoxide, and of Fe_3O_4 0.86 x 10^{-5} M were prepared. Different concentrations of magnetite nanoparticles were obtained by taking 1, 2, 3, 4, 5ml of stock solution diluted to 10 ml to give (0.86, 1.72, 2.58, 3.44, 4.30) x 10^{-4} M respectively. 1ml of cisplatin stock solution sonicacted for 2 min with different concentration of Fe_3O_4 nanoparticles ,respectively and measured by UV-visible absorption and emission techniques.

2.3 Equipment

Thermal gravimetric analysis (TGA) curve of the air dried precursor was obtained with a thermogravimetriy-differential thermal analyzer (Shimadzu TGA-50), using platinum crucible with 2.1 mg of the precursor sample under a continuous nitrogen flow (15 ml/ min), at a heating rate of 10 °C/min. UV-visible absorption spectra were measured on a Shimadzu UV-2450 spectrophotometer. Fluorescence spectra were recorded on a Shimadzu RF-5301PC spectrofluorometer. The Fourier- transform infrared (FTIR) spectra were measured with a JASCO spectrometer 4100 using the KBr pellet technique. The X-ray diffraction (XRD) measurements were recorded by an X- ray diffractometer Shimadzu XRD-6000, equipped with CuKα radiation (λ = 1.54056 Å). The morphological feature of the Fe_3O_4 nanoparticles was observed by a scanning electron microscope (FESEM, JEOL, JSM-6360 LA, the samples were coated with gold), Transmission electron micrographs (TEM) were obtained using Tecnai G20, Super twin, double tilt, FEI, Nertherland operating at an accelerating voltage of 200 kV.

3.Results and discussion

Characterization of synthesized nanoparticles Fe_3O_4 NPs:

Formation mechanism of magnetite nanoparticles:

Magnetite nanoparticles were synthesized as shown in Scheme (2). Fe^{+2} and Fe^{+3} are hydrolyzed and converted to hydroxide compounds. The hydroxide compounds have been crystallized to Fe_3O_4 slowly by addition of strong base, and the combination between hydroxides by molar ratio 1:2, respectively.

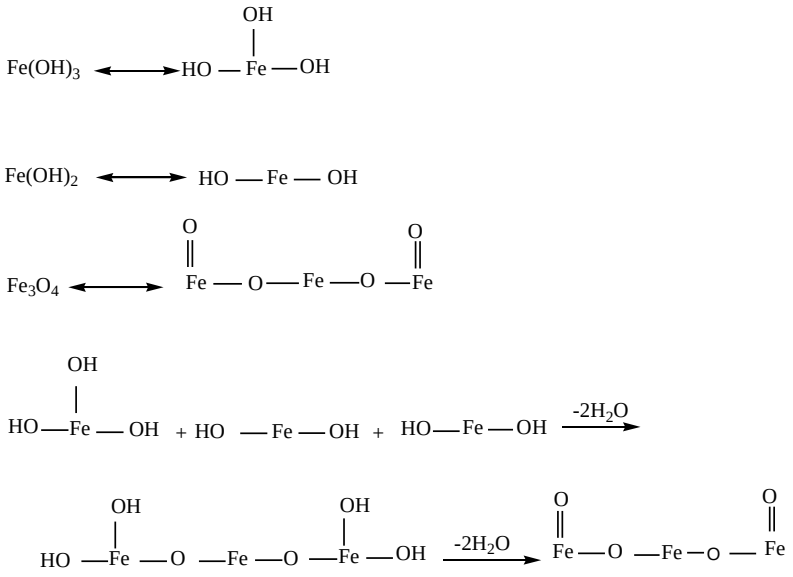

Scheme (2) Formation mechanism of Fe_3O_4 nanopaticles.

Structure characterization:
Xray analysis:

Figure (1) shows XRD pattern of MNP .the pattern confirms the major composition of magnetite, the sites of the diffraction peaks are 30^0, 35.24^0, 42.9^0, 53.9^0, 57^0, and 62.8^0. Which are the same as the reference for standard sample [32], and relative to those from the JCPDS card (19-0629) for magnetite synthesis. Wide peaks are related to the small size of particles. The diffraction peaks are broadened owing to small crystallite size all the observed diffraction peaks could be indexed by cubic structure of Fe_3O_4.
The crystallite size calculated from the FWHM(full width and half maximum) by applying Debye-Scherrer formula[33] eqn (1) was found to be 16.64 nm. The most intense peak (311) was used for the crystallite size evaluation.

$$D_{hkl} = 0.9\lambda/(\beta \cos\theta) \quad \textbf{(1)}$$

Where β is the full-width at half-maximum, the wavelength λ = 0.154056 nm, θ is the half diffraction angle of 2θ.

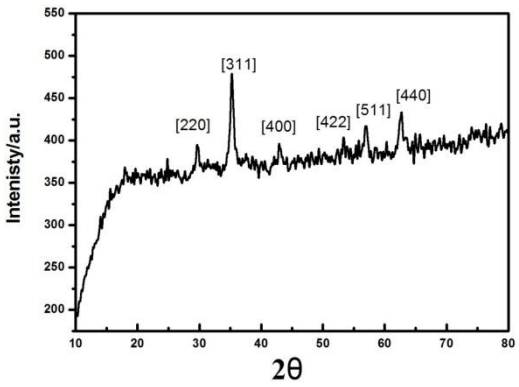

Fig (1) XRD image of the investigated magnetite nanoparticles.

TEM and SEM analysis

The size and morphology of the Fe_3O_4 were characterized by TEM and SEM. Fig. 2a, 2b Images show spherical shape of magnetite nanoparticles with size from 10nm to 20nm as the following table .the size calculated by Debye-Scherrer equation(16.64 nm) is in the range which calculated by TEM analysis.

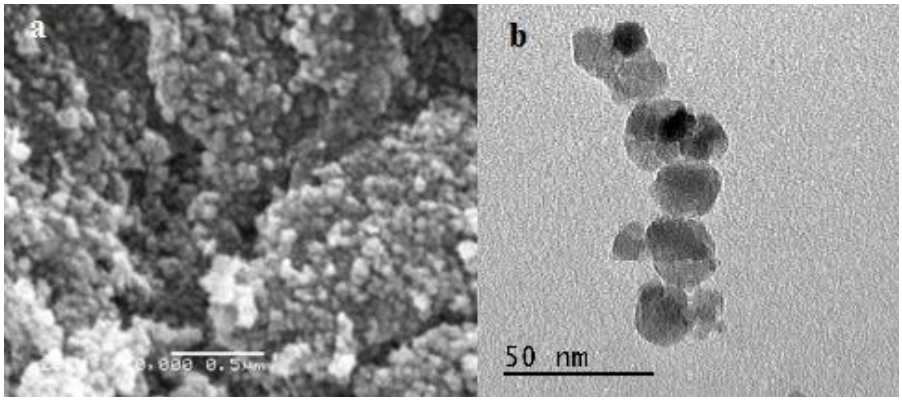

Fig (2) shows SEM image of investigated Fe_3O_4 nanoparticles(a), TEM image(b).

Table (1) different size and number of particles of the investigated Fe_3O_4 NPs.

Number of particles	Size / nm
2	10.1
4	14.8
2	18.5
2	20.3

Thermal gravimetric analysis

Figure (3) shows thermal gravimetric analysis of magnetite nanoparticles. The figure shows low weight loss percent ratio ≈ 3.6% which refers to high stability and purification of the magnetite nanoparticles. This little loss in weight due to the humidity or ammonia adsorbed on the surface of MNP.

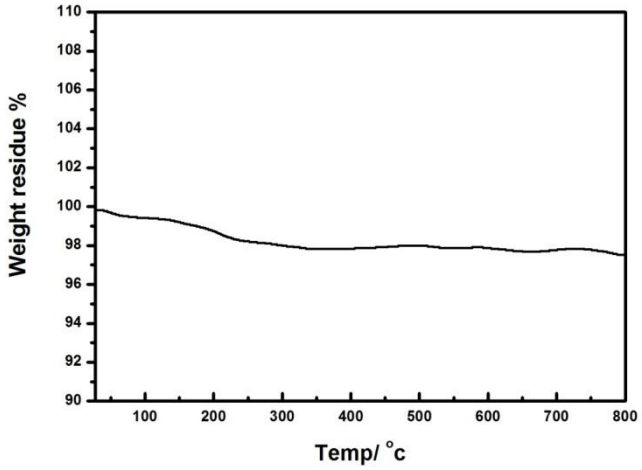

Fig (3) Thermal gravimetric analysis of Fe_3O_4 nanoparticles.

FTIR spectra analysis

Figure (4) shows the FTIR spectra of the magnetite nanoparticles. The spectra shows strong absorption bands around 585 cm^{-1}charecterized for Fe^{+3}-O^{-2} and weak band around 426 cm^{-1} corresponding to Fe^{+2}-O^{-2}. These corroborate that the main phase of as-prepared particles is magnetite [34]. The absorption band at 1622 cm^{-1} refers to the vibration of remainder H_2O in the sample [35].

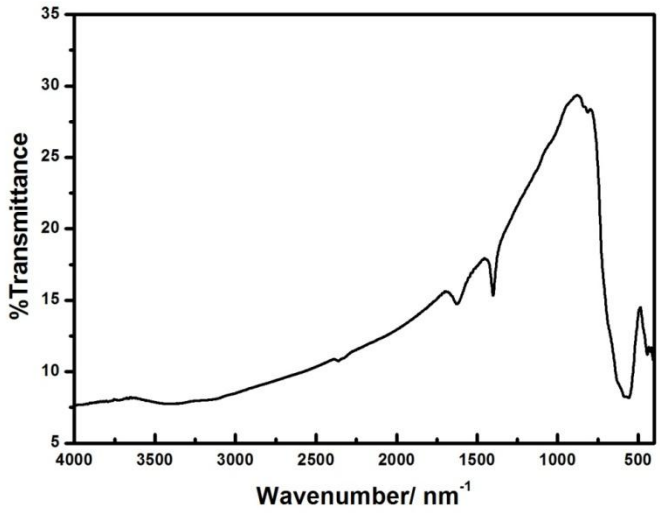

Fig (4) FTIR spectra of Fe_3O_4 nanoparticles.

Absorption Spectra

Figure (5) shows the absorption spectrum of cisplatin of concentration ($41x10^{-3}$ M) in the absence and presence of different concentrations of Fe_3O_4 in dimethylsulphoxide DMSO at room temperature with an incident absorption spectrum of cisplatin anticancer drug. It is apparent that upon adding different concentration of Fe_3O_4 within ranges ($0 – 4.30 x10^{-4}$ M) to cisplatin leads to a consistent enhancement without any shift of the absorbance. This influence is probably due to the adsorption of some drug molecules on the surface of the $Fe_3O_4$and formation of the ground state complex located at 285 nm.

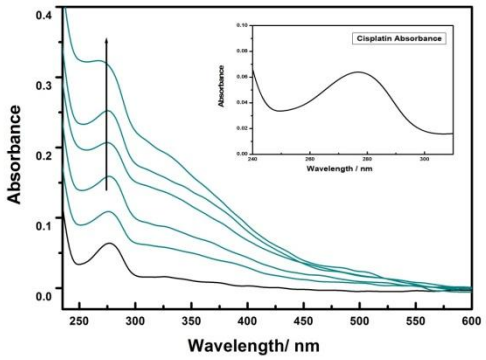

Fig (5) Absorption spectra of cisplatin drug in absence and presence of Fe_3O_4 NPs with incident absorption spectrum of cispaltin drug.

The equilibrium for the association of cisplatin with Fe_3O_4 can be expressed as:

$$CIS + Fe_3O_4 \overset{K_{app}}{\Longleftrightarrow} CIS \ldots\ldots Fe_3O_4 \quad (2)$$

Where K represents the apparent association constant which defined as:

$$K = \frac{CIS \ldots\ldots Fe_3O_4}{[CIS][Fe_3O_4]} \quad (3)$$

K value can be obtained by Benesi and Hildebrand equation[36] :

$$\frac{1}{A_{obs} - A_o} = \frac{1}{A_C - A_o} + \frac{1}{K_{app}\,(A_C - A_o)[Fe_3O_4]} \quad (4)$$

Where A_o and A_c are the absorbances of cisplatin and the complex at 285nm. A_{obs} is the observed absorbance of the solution containing different concentrations of Fe_3O_4 NP.

Figure (6) depicts a linear plot of 1/ (A_{obs}–A_o) as a function of reciprocal concentration of Fe_3O_4. The estimated value of the association constant (K_{app}) determined from this linear plot is $4x10^2$ M^{-1} with a good correlation coefficient (R^2= 0.99477).

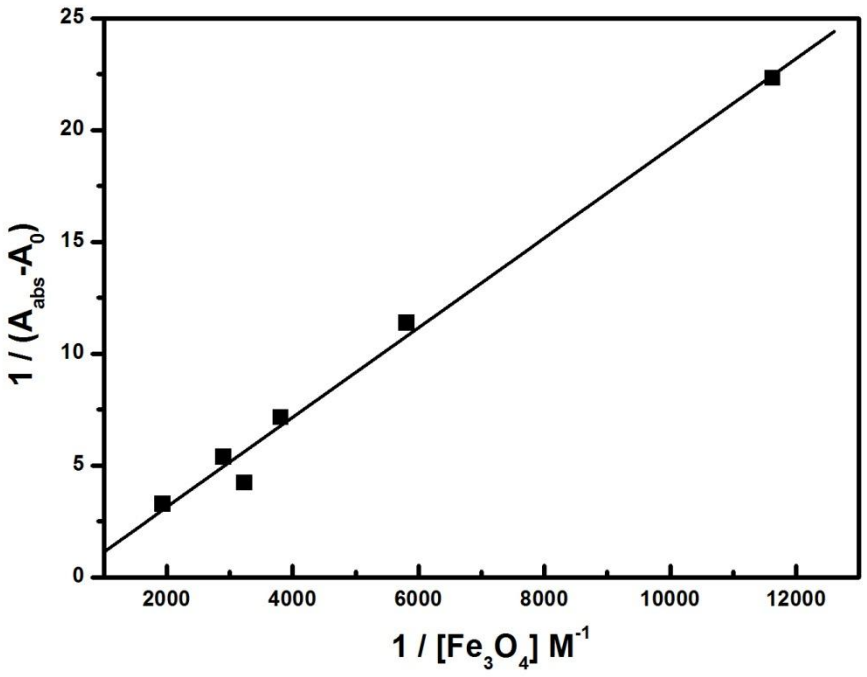

Fig (6) plot of 1/ (A_c-A_o) versus the reciprocal concentration of Fe_3O_4.

Fluorescence quenching studies

Figure (7) shows the emission spectra of cisplatin in absence and presence of different concentrations of Fe_3O_4 nanoparticles. Upon addition of Fe_3O_4 nanoparticles, the flourescence intensity of cisplatin decreases, however no new emission band was detected, indicating the absence of exciplex formation.

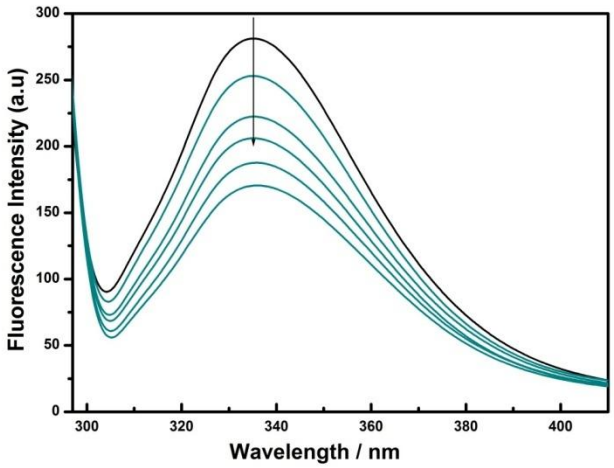

Fig (7) Fluorescence quenching of cisplatin in presence and absence of Fe_3O_4 (λ_{ex}=285 nm).

The second-order quenching rate constant k_q was determined from the well-known Stern–Volmer (SV) **equation (5)**

$$I_o/I = 1 + K_{SV}[Q] = K_q\tau_o[Q] \quad (5)$$

Where I_o and I are the relative fluorescence intensities of cisplatin drug in absence and presence of quencher concentration [Q], and K_{sv} is Stern-Volmer constant. k_q is the second order quenching rate constant and τ_o is the fluorescence lifetime of the fluorophore in the absence of quencher.

A linear plot of I_o/I versus quencher concentration is shown in **Fig (8)** and from the slope of plot, K_{SV} was found to be $3.922x10^2$ M^{-1}. Their values are close to that determined from the absorption spectra.

The values of quenching rate constant (k_q) are determined from K_{SV} value using $K_{sv} = k_q\tau_o$. At room temperature, the observed fluorescence lifetime of cisplatin is τ_o = 2.03 ns [37]. Therefore, according to **equation (5)**, the estimated k_q value equals to$1.93x10^{11}$ $M^{-1}s^{-1}$. The higher quenching rate constant values suggesting that the quenching is static in nature.

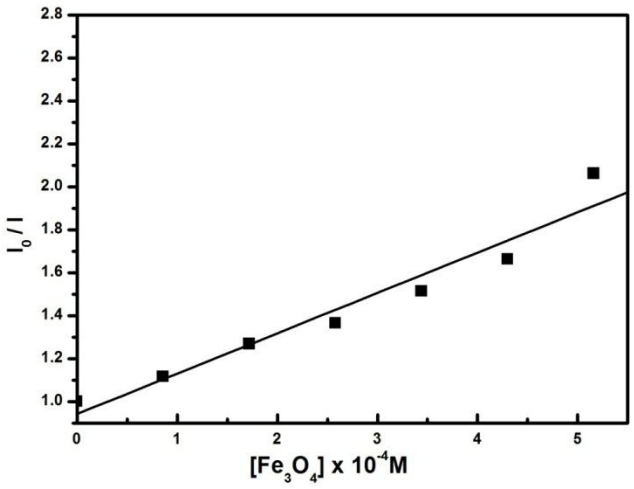

Fig (8) Stern-Volmer plot for cisplatin ($41x\ 10^{-3}$ M) in presence and absence of Fe_3O_4 nanoparticles (λ_{ex}=285 nm)

Binding constant and binding sites

The static quenching can be a valuable source for determination the binding constant (*K*) resulted from the formation of ground state complex between the fluorophore (cisplatin drug) and the quencher (Fe_3O_4 NP) by using the method of linear regression according to the relation [38]:

$$log\left[\frac{I_0-I}{I}\right] = \log K + nlog[Q] \quad (6)$$

Where *n* is the number of binding sites and *K* is the binding constant between cisplatin and Fe_3O_4 NP. Figure (9) shows linear regression analysis of log $[(I_0 - I)/I]$ versus *log* [*Q*] on the basis of relation (6) leads to estimation of K value from the slope and intercept of the plot. From the data, we observed that the value of *n* almost close to 1, and it indicates that there is only one type of interaction between cisplatin and Fe_3O_4 NP. It is apparent that the values of binding constant obtained from the fluorescence data matches well with that determined from the absorption data. The good agreement between these values of binding constant highlighted the validity of assumption proposed for the association between cisplatin and Fe_3O_4 NP.

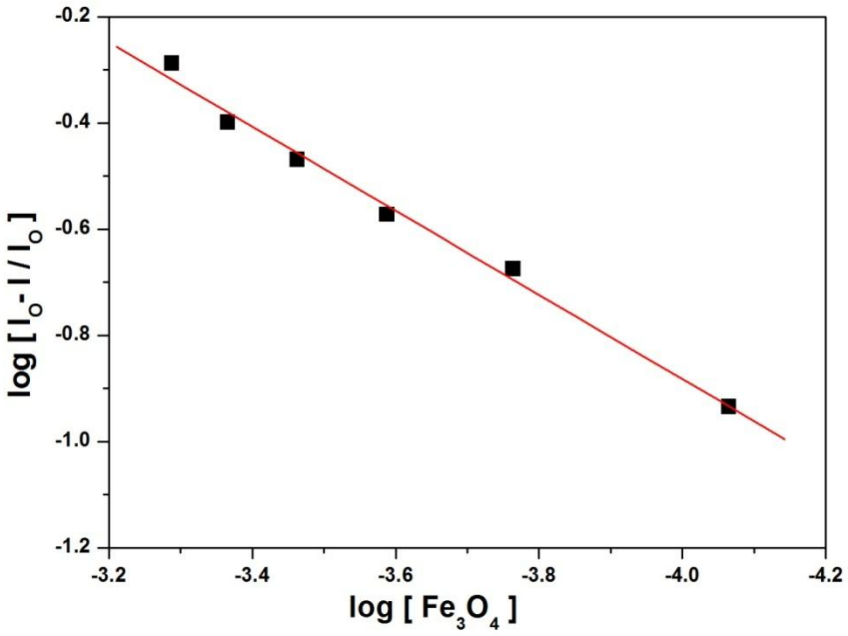

Fig (9) The plot of log $[(I_0 - I)/I]$ versus log [Q] for cisplatin quenching by Fe_3O_4 NP.

Reference

[1] N. Lee, T. Hyeon, Designed synthesis of uniformly sized iron oxide nanoparticles for efficient magnetic resonance imaging contrast agents, Chem. Soc. Rev. 41 (2012) 2575–2589.

[2]] L. Bu, J. Xie, K. Chen, J. Huang, Z.P. Aguilar, A. Wang, K.W. Sun, M.S. Chua, S. So, Z. Cheng, H.S. Eden, B. Shen, X. Chen, Assessment and comparison of magnetic nanoparticles asMRI contrast agents ina rodentmodel of human hepatocellular carcinoma, Contrast Media Mol. Imaging 7 (2012) 363–372.

[3] S.A. Corr, S.J. Byrne, R. Tekoriute, C.J. Meledandri, D.F. Brougham, M. Lynch, C. Kerskens, L. O'Dwyer, Y.K. Gun'ko, Linear assemblies of magnetic nanoparticles as MRI contrast agents, J. Am. Chem. Soc. 130 (2008) 4214–4215.

[4] M.V. Yigit, A. Moore, Z. Medarova, Magnetic nanoparticles for cancer diagnosis and therapy, Pharm. Res. 29 (2012) 1180–1188.

[5]] R. Tietze, S. Lyer, S. Durr, C. Alexiou, Nanoparticles for cancer therapy using magnetic forces, Nanomedicine (Lond.) 7 (2012) 447–457.

[6]] C. Li, L. Li, A.C. Keates, Targeting cancer gene therapy with magnetic nanoparticles, Oncotarget 3 (2012) 365–370.

[7]Lu AH, Salabas EL, Schüth F. Magnetic nanoparticles: synthesis, protection, functionalization, and application.Angew Chem Int Ed. 2007;46(8):1222–1244

[8] Zubarev AY, Iskakova LY. To the theory of rheological properties of ferrofluids: influence of drop-like aggregates. Physica A. 2004;343:65–80

[9] Rossi LM, Silva FP, Vono LLR, et al. Superparamagnetic nanoparticlesupported palladium: a highly stable magnetically recoverable and reusable catalyst for hydrogenation reactions. Green Chem. 2007;9(4):379–385.

[10] Lee JH, Jun Y, Yeon SI, Shin JS, Cheon J. Dual-mode nanoparticle probes for high-performance magnetic resonance and fluorescence imaging of neuroblastoma. Angew Chem Int Ed Engl. 2006;118(48):8340–8342.
[11] Hu FQ, Wei L, Zhou Z, Ran YL, Li Z, Gao MY. Preparation of biocompatible magnetite nanocrystals for in vivo magnetic resonance detection of cancer. Adv Mater. 2006;18(19):2553–2556.
[12] Nasongkla N, Bey E, Ren J, et al. Multifunctional polymeric micelles as cancer-targeted, MRI-ultrasensitive drug delivery systems. Nano Lett. 2006;6(11):2427–2430.
[13] Wu W, He Q, Jiang C. Magnetic iron oxide nanoparticles: synthesis and surface functionalization strategies.Nanoscale Res Lett. 2008;3(11):397–415
[14] Salehizadeh H, Hekmatian E, Sadeghi M, Kennedy K. Synthesis and characterization of core-shell Fe_3O_4-gold-chitosan nanostructure. J Nanobiotechnol. 2012;10(1):1–7.
[15] Park HY, Schadt MJ, Wang L, et al. Fabrication of magnetic core@ shell Fe oxide@ Au nanoparticles for interfacial bioactivity and bioseparation. Langmuir. 2007;23(17):9050–9056.
[16] Sonvico F, Mornet S, Vasseur S, et al. Folate-conjugated iron oxide nanoparticles for solid tumor targeting as potential specific magnetic hyperthermia mediators: synthesis, physicochemical characterization, and in vitro experiments. Bioconjug Chem. 2005;16(5):1181–1188.
[17] Teo, B.M.; Chen, F.; Hatton, T.A.; Grieser, F.; Ashokkumar, M. Novel one-pot synthesis ofmagnetite latex nanoparticles by ultrasound irradiation. Langmuir 2009, 25, 2593–2595.
[18] Teja, A.S.; Koh, P. Synthesis, properties, and applications of magnetic iron oxidenanoparticles. Prog. Cryst. Growth Charact. Mater. 2009, 55, 22–45
[19] Sun, S.; Zeng, H. Size-controlled synthesis of magnetite nano-particies. J. Am. Chem. Soc. 2002, 124, 8204–8205.
[20] Peng, S.; Wang, C.; Xie, J.; Sun, S. Synthesis and stabilization of monodisperse Fe nanoparticles. J. Am. Chem. Soc. 2006, 128, 10676–10677.
[21] Ge, J.; Hu, Y.; Biasini, M.; Dong, C.; Guo, J.; Beyermann, W.P.; Yin, Y. One-step synthesis of highly water-soluble magnetite colloidal nanocrystals. Chem. Eur. J. 2007, 13, 7153–7161.
[22] Lu, X.; Niu, M.; Qiao, R.; Gao, M. Superdispersible PVP-coated Fe3O4 nanocrystalsprepared by a “one-pot” reaction. J. Phys. Chem. B 2008, 112, 14390–14394.
[23] Li, Z.; Chen, H.; Bao, H.; Gao, M. One-pot reaction to synthesize water-soluble magnetite nanocrystals. Chem. Mater. 2004, 16, 1391–1393.
[24] . Vargas, J.M.; Zysler, R.D. Tailoring the size in colloidal iron oxide magnetic nanoparticles. Nanotechnology 2005, 16, 1474–1476.
[25] Hu, D.; Wang, Y.; Song, Q. Weakly magnetic field-assisted synthesis of magnetite nanoparticles in oxidative co-precipitation. Particuology 2009, 7, 363–367.
[26] Mizukoshi, Y.; Shuto, T.; Masahashi, N.; Tanabe, S. Preparation of superparamagneticmagnetite nanoparticles by reverse precipitation method: Contribution of sonochemicallygenerated oxidants. Ultrason. Sonochem. 2009, 16, 525–531.
[27] Nedkov, I.; Merodiiska, T.; Slavov, L.; Vandenberghe, R.E.; Kusano, Y.; Takada, J. Surfaceoxidation, size and shape of nano-sized magnetite obtained by coprecipitation. J. Magn. Magn. Mater. 2006, 300, 358–367.
[28] Qu, S.; Yang, H.; Ren, D.; Kan, S.; Zou, G.; Li, D.; Li, M. Magnetite nanoparticles prepared byprecipitation from partially reduced ferric chloride aqueous solutions. J. Colloid Interf. Sci. 1999, 215, 190–192.
[29] Pardoe, H.; Chua-anusorn, W.; Pierre, T.G.S.; Dobson, J. Structural and magnetic properties of nanoscale iron oxide particles synthesized in the presence of dextran or polyvinyl alcohol. J. Magn. Magn. Mater. 2001, 225, 41–46.
[30] Bandhu, A.; Mukherjee, S.; Acharya, S.; Modak, S.; Brahma, S.K.; Das, D.; Chakrabarti, P.K. Dynamic magnetic behavior and Mössbauer effect measurements of magnetite nanoparticles prepared by a new technique in the co-precipitation method. Solid State Commun. 2009, 149, 1790–1794
[31] Ozkaya, T.; Toprak, M.S.; Baykal, A.; Kavas, H.; Koseoglu, Y.; Aktas, B. Synthesis of Fe3O4 nanoparticles at 100 °C and its magnetic characterization. J. Alloys Compd. 2009, 472, 18–23.
[32] B.Wang1 , Q.Wei2 , Sh.Qu1, Synthesis and Characterization of Uniform and Crystalline Magnetite Nanoparticles via Oxidation-precipitation and Modified co-precipitation Methods, IJ of ELECTROCHEMICAL SCIENCE, (2013) 3786 – 3793.
[33] B.D. Cullity, Elements of X-ray Diffraction, A.W.R.C. Inc., Massachusetts, 1967.
[34] R.M. Cornell, U. Schwertmann, The Iron Oxides: Structure, Properties,
Reactions, Occurrence and Uses, second ed., Wiley–VCH, Weinheim,
2003.
[35]] T. Rajh, L.X. Chen, K. Lukas, T. Liu, M.C. Thurnauer, D.M. Tiede,

J. Phys. Chem. B 106 (2002) 10543.
[36] H.A. Benesi, J.H. Hildebrand, J. Am. Chem. Soc. 71 (1949) 2703.
[37] S. Kim, J.Jeong, Y.park, J.Song, A.Kim, J.Yong Choi, W.Sik Chae, 4-hexylresorcinol inhibits transglutaminase-2 activity and has synergistic effects along with cisplatin in KB cells, oncology reports 25 (2011) 1597-1602.
[38] M. Asha Jhonsi, A. Kathiravan, R. Renganathan, Spectroscopic studies on the interaction of colloidal capped CdS nanoparticles with bovine serum albumin, Colloids and Surfaces B: Biointerfaces 72 (2009) 167–172.